Supporting Information

Positron Emission Tomography Imaging of Staphylococcus aureus Infection Using a Nitro-Prodrug Analog of 2-[18F]F-p-Aminobenzoic Acid

Yong Li,[†,‡,£] Fereidoon Daryaee,[†,‡,£] Grace E. Yoon,[‡,⊥] Doyoung Noh,[‡,⊥] Peter M Smith-Jones,[⊥] Yuanyuan Si,[‡] Stephen G. Walker,[§] Nashaat Turkman,[¶] Labros Meimetis,[£] and Peter J. Tonge[†,‡,¶,£,*]

[†]Center for Advanced Study of Drug Action, and Departments of [‡]Chemistry, [¶]Radiology, Stony Brook University, 100 Nicolls Road, 633 Chemistry, Stony Brook, New York 11794, United States

[§]Department of Oral Biology and Pathology, Stony Brook University, Stony Brook, NY 11794-3400, United States

[⊥]The Facility for Experimental Radiopharmaceutical Manufacturing, Department of Psychiatry, Stony Brook University, Stony Brook, New York 11794, United States

[£] Chronus Pharmaceuticals, 25 Health Sciences Drive, Stony Brook, New York, 11790-3350

*Corresponding Author E-mail: peter.tonge@stonybrook.edu

Table of Contents

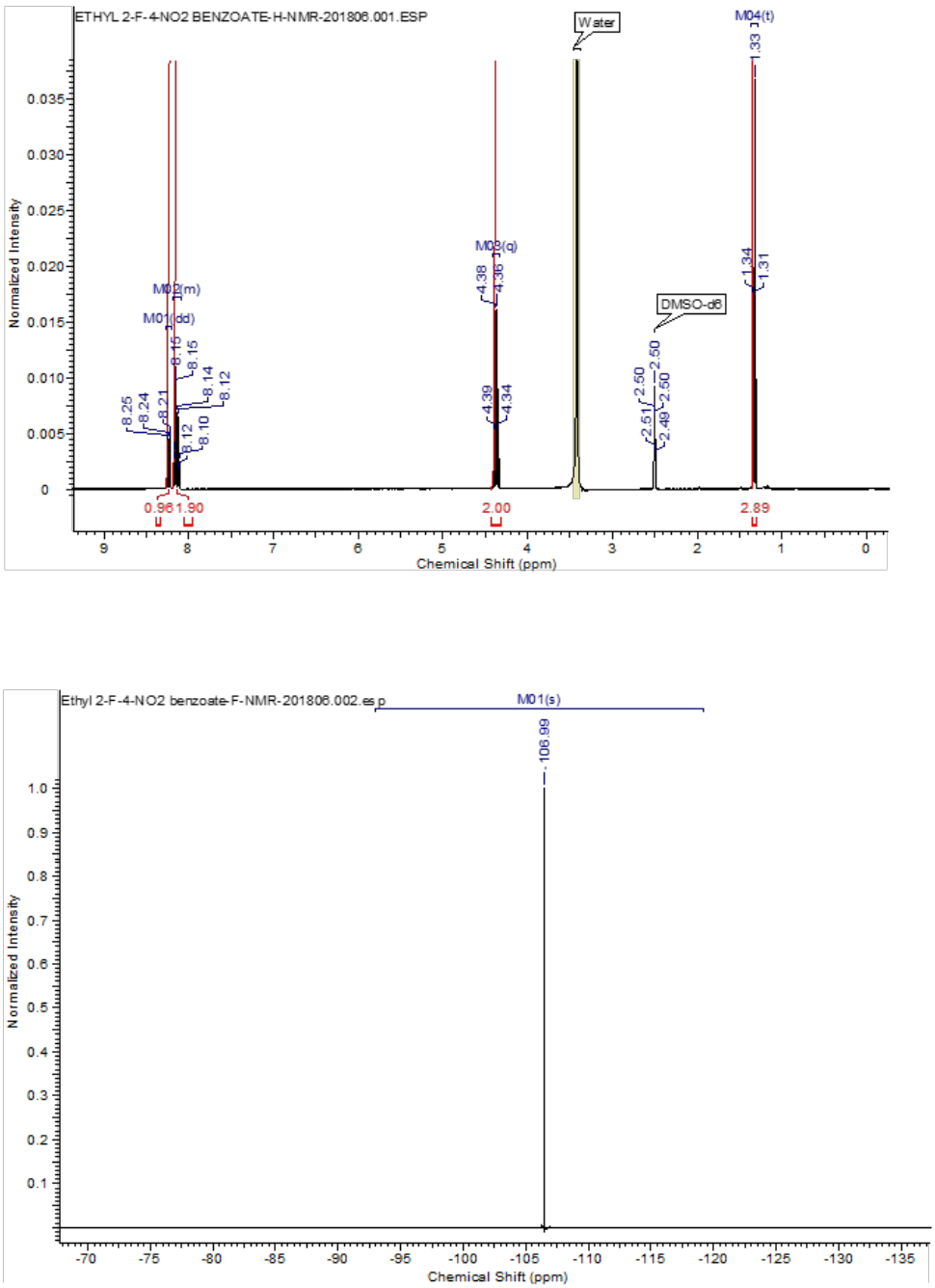

Figure S1. H-NMR and F-NMR of 2-F-ENB

<u>Ethyl 2-fluoro-4-nitro benzoate:</u> ^{1}H NMR (400 MHz, DMSO-d_6) δ ppm 1.33 (t, J=7.09 Hz, 3 H) 4.37 (q, J=7.09 Hz, 2 H) 8.09 - 8.19 (m, 2 H) 8.23 (dd, J=10.51, 1.71 Hz, 1 H). ^{19}F NMR (376 MHz, DMSO-d_6) δ ppm -106.99 (s, 1 F)

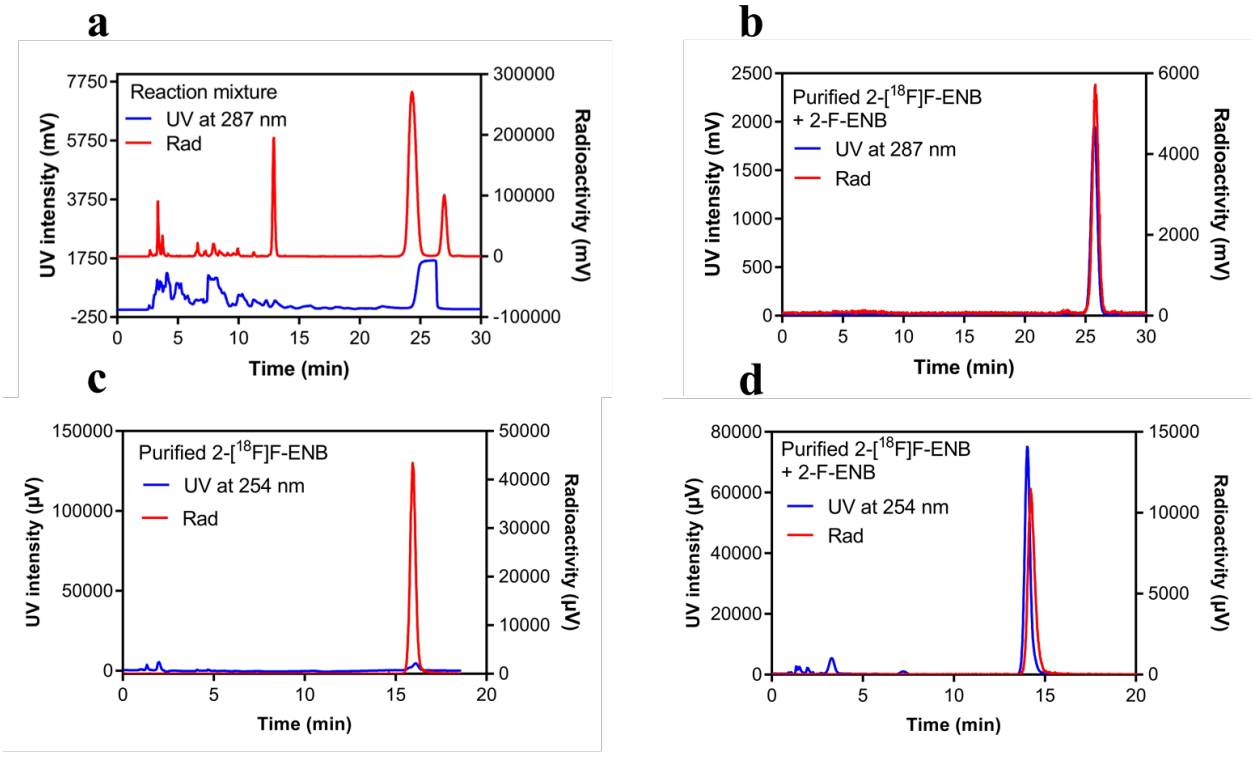

	Manual Synthesis (n=8)	Automated synthesis (n=2)
Decay-corrected radiochemical yield (%)	7.0 ± 0.8	29 ± 4
Radiochemical purity (%)	99.2 ± 0.7 %	98.5 ± 0.3 %
Specific activity	3983 ± 1704 mCi/µmole	2556 ± 904 mCi/µmole

Figure S2. HPLC trace of 2-[^{18}F]F-ENB prepared manually and by automated synthesis

(a) Semi-preparative HPLC chromatography of manually-synthesized 2-[^{18}F]F-ENB using a Phenomenex Luna 10 µm C18(2) column (250 x 10 mm) with 45% MeCN/55% H_2O as the eluent. The flow rate 4 mL/min. The blue trace is the UV absorption of the eluent at 287 nm and the red trace is the radioactive signal.

(b) Analytical HPLC of a co-injection of the 2-F-ENB cold standard with purified 2-[^{18}F]F-ENB prepared by manual synthesis. The blue trace is the UV absorption of the eluent at 287 nm, and the red trace is the radioactive signal.

(c) Analytical HPLC chromatography of purified 2-[^{18}F]F-ENB prepared by automated synthesis using a Phenomenex Luna 10 μm C18(2) column (250 x 10 mm) with 45% MeCN/55% H_2O as the eluent. The flow rate 0.8 mL/min. The blue trace is the UV absorption of the eluent at 254 nm, and the red trace is the radioactive signal.

(d) Analytical HPLC of a co-injection of the 2-F-ENB cold standard with purified 2-[^{18}F]F-ENB prepared by automated synthesis. The blue trace is the UV absorption of the eluent at 254 nm, and the red trace is the radioactive signal.

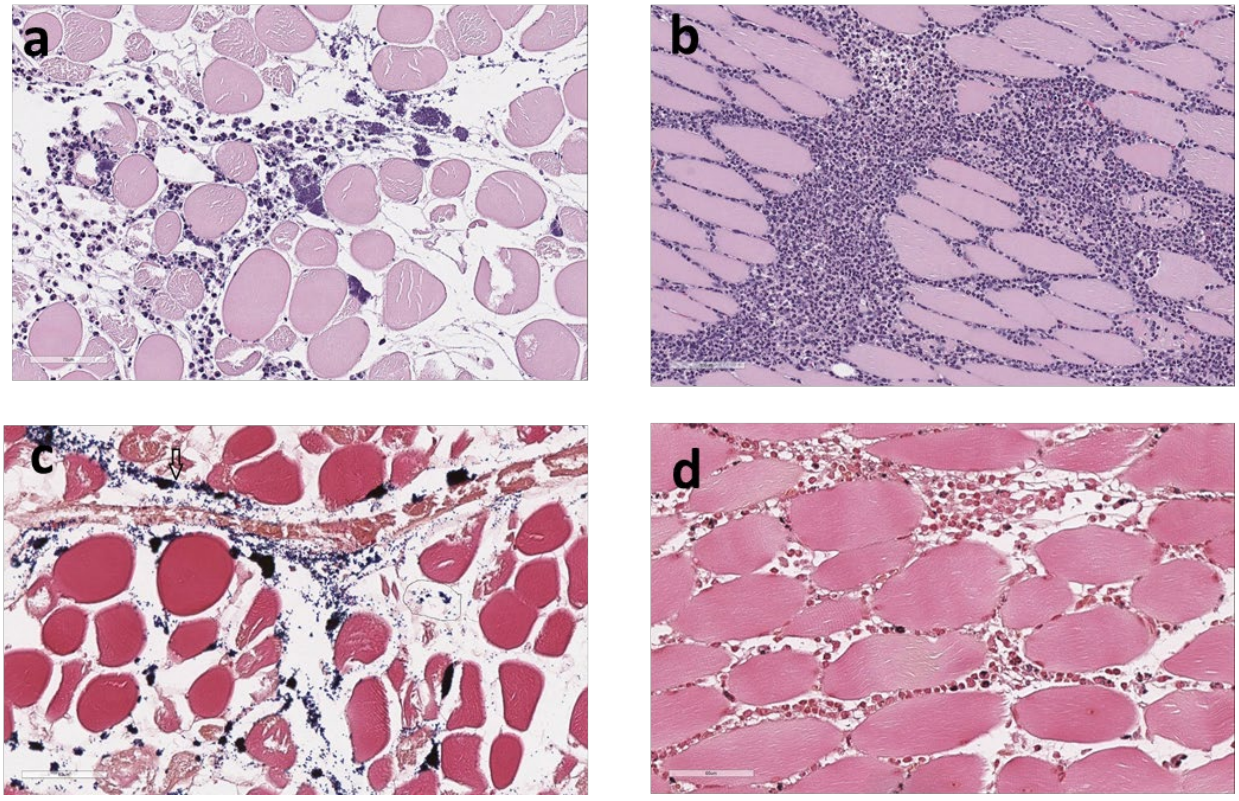

Figure S3. Histology of *S. aureus* Newman infection and sterile inflammation in the rat model. (a) H&E staining of *S. aureus*-infected triceps. (b) H&E staining of triceps with sterile inflammation (heat-killed *S. aureus*). (c) Gram stain of infected triceps showing Gram-positive cocci in clusters. (d) Gram stain of inflamed triceps showing that no Gram-positive cocci are found.

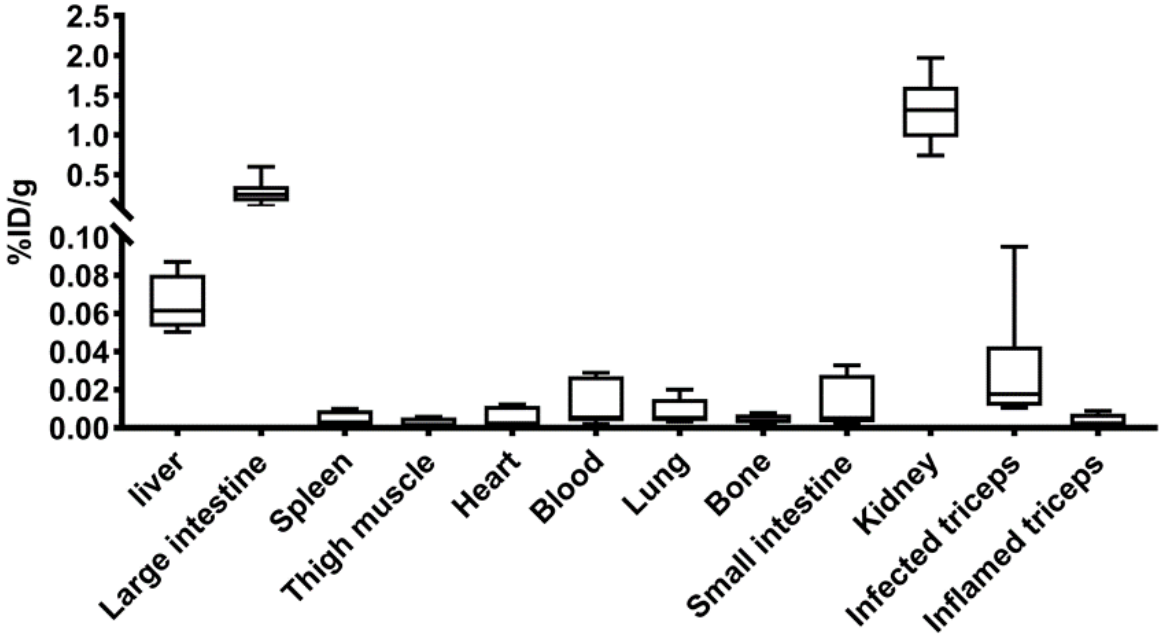

Figure S4. Post-mortem analysis of 2-[^{18}F]F-ENB distribution. After the animals were injected IV with 2-[^{18}F]F-ENB and scanned for 180 min, they were euthanized, and the tissues weighed and harvested for automated gamma counting. Data are medians with interquartile and ranges are shown (n=6).

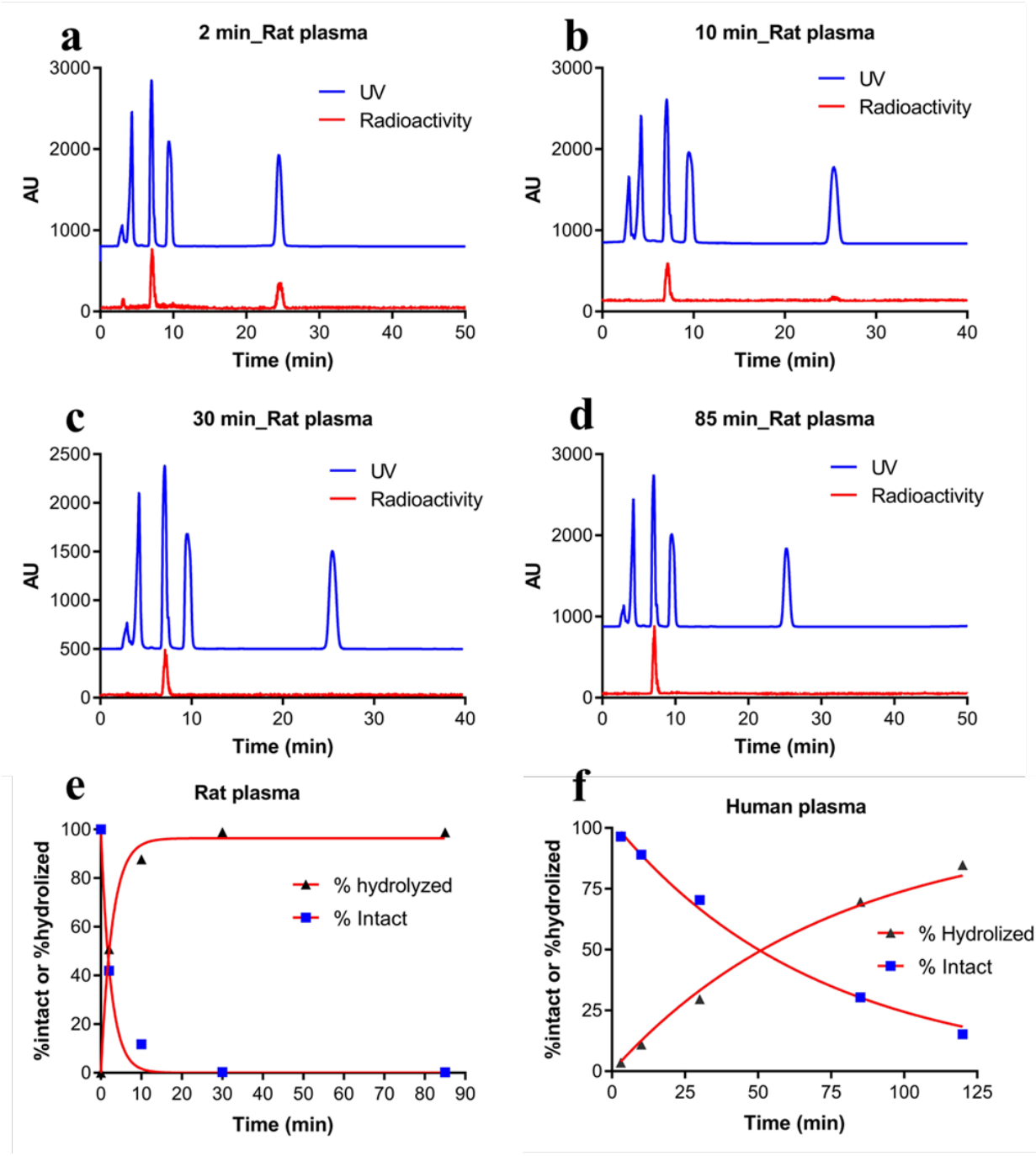
a
2 min_Rat plasma
UV
Radioactivity
AU
Time (min)
b
10 min_Rat plasma
UV
Radioactivity
AU
Time (min)
c
30 min_Rat plasma
UV
Radioactivity
AU
Time (min)
d
85 min_Rat plasma
UV
Radioactivity
AU
Time (min)
e
Rat plasma
% hydrolyzed
% Intact
%intact or %hydrolized
Time (min)
f
Human plasma
% Hydrolized
% Intact
%intact or %hydrolized
Time (min)

Figure S5. In vitro metabolic stability of 2-[^{18}F]F-ENB in rat and human plasma. (a-d) HPLC traces of metabolites of 2-[^{18}F]F-ENB incubated with rat plasma at different time points (2 min, 10 min, 30 min, 85 min) and spiked with cold standards. (e) The metabolic half-life of 2-[^{18}F]F-ENB in rat plasma was calculated by fitting the percentage of either intact tracer or metabolites generated in human plasma as the function of time to a single exponential equation. (f) The metabolic half-life of 2-[^{18}F]F-ENB in human plasma was calculated by fitting the percentage of either intact tracer or metabolites generated in human plasma as the function of time to a single exponential equation. 2-[^{18}F]F-ENB has longer half-life in human plasma ($t_{1/2}$ = 35 min) than in rat plasma ($t_{1/2}$ = 2 min).

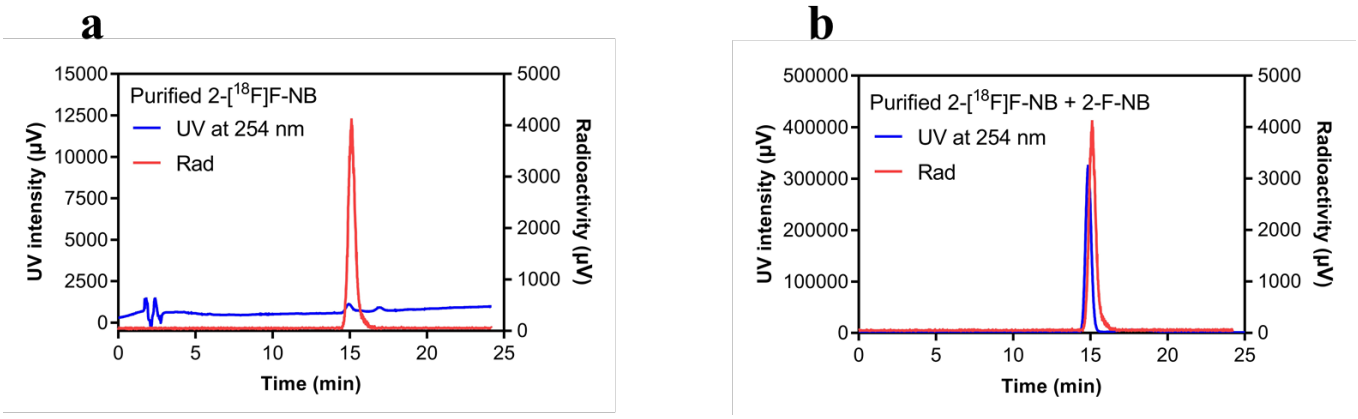

	Automated synthesis (n=1)
Decay-corrected radiochemical yield	26 %
Radiochemical purity	99.2 %
Specific activity	1110 mCi/μmole

Figure S6. Analytical HPLC of 2-[^{18}F]F-NB prepared by automated synthesis

(a) Analytical HPLC chromatography of purified 2-[^{18}F]F-NB prepared by automated synthesis using a Phenomenex Luna 10 μm C18(2) column (250 x 10 mm) with 25% MeCN/75% H_2O with 0.1% TFA as the eluent. The flow rate 0.8 mL/min. The blue trace is the UV absorption of the eluent at 254 nm, and the red trace is the radioactive signal.

(b) Analytical HPLC of a co-injection of the 2-F-NB cold standard with purified 2-[^{18}F]F-NB prepared by automated synthesis. The blue trace is the UV absorption of the eluent at 254 nm, and the red trace is the radioactive signal.

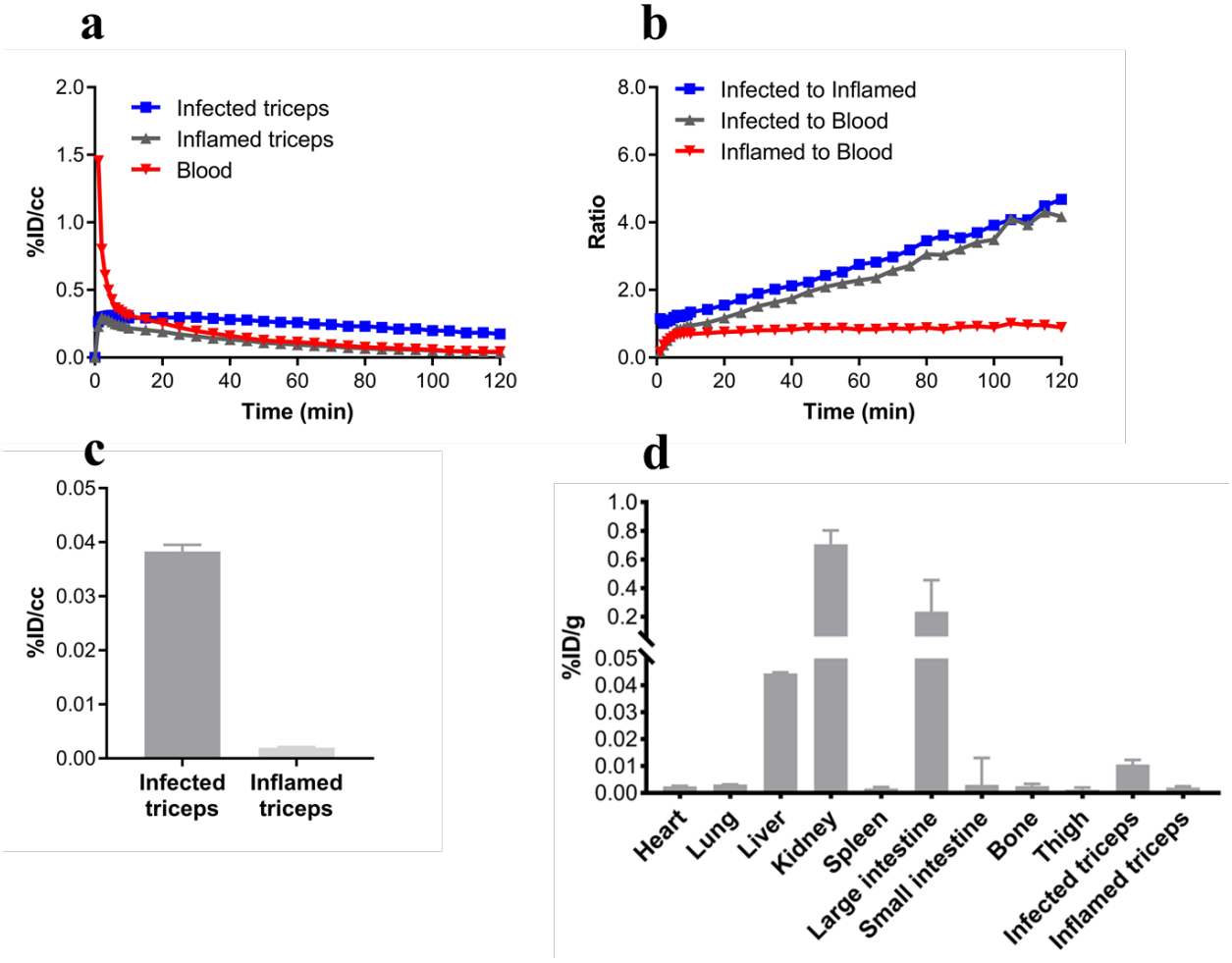

Figure S7. Time activity curve (TAC) in infected triceps, inflamed triceps and blood and biodistribution of 2-[^{18}F]F-NB in major organs. (a) The right triceps of the rats were infected with *S. aureus* Xen 29 and the left triceps were injected with a 10-fold higher burden of heat-killed *S. aureus* to induce sterile inflammation. The rats were scanned by PET/CT for 120 min (rats with sterile inflammation in the left triceps) immediately starting from tracer administration. The PET scan was separated into ten frames (1-min) and twenty-two frames (5-min). TACs of infected triceps (blue), inflamed triceps (grey) and blood (left heart ventricle, red) are shown. Data represented as mean with standard error of the mean (n=4). (b) Time-dependent accumulation of 2-[^{18}F]F-NB in infected and inflamed triceps compared to the blood (left heart ventricle). Data are

presented as the mean and standard error of the mean (n = 4). (c) Comparison of 2-[^{18}F]F-NB accumulation in the infected triceps and inflamed triceps 180-200 min after tracer injection (n = 3). (d) Post-mortem ex vivo analysis of 2-[^{18}F]F-NB biodistribution, represented as % injected dose per gram (%ID/g). After the animals were injected IV with 2-[18F]F-NB and scanned for 180 min, they were sacrificed and the tissues and major organs weighed and harvested for automated gamma counting. Data represented as mean with standard error of the mean (n=3).

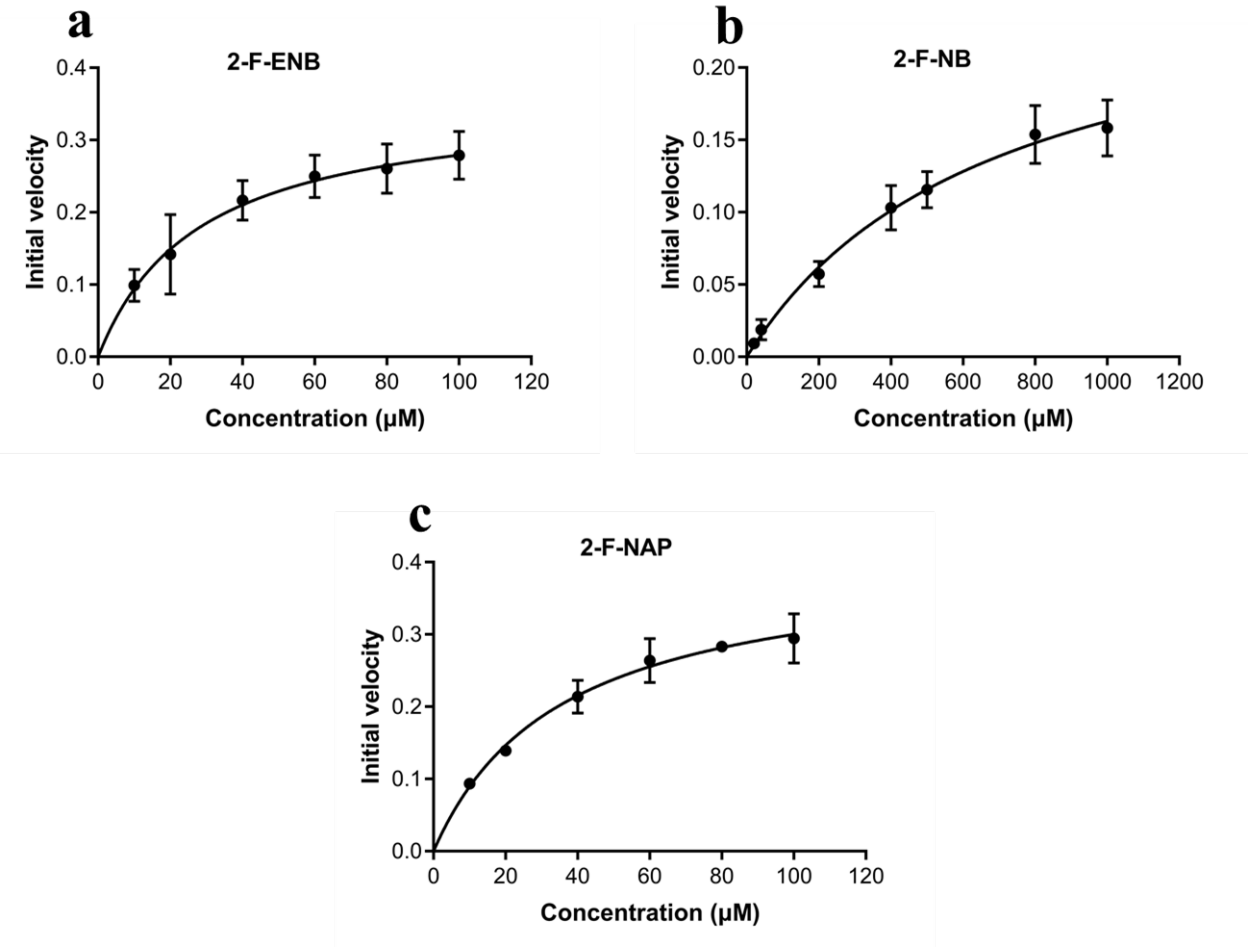

Figure S8. Kinetics of 2-F-ENB , 2-F-NB and 2-F-NAP reduction by NfsB.

The kinetics for the reduction of ethyl 2-fluoro-*p*-nitrobenzoate (F-ENB)(a), 2-fluoro-*p*-nitrobenzoate (F-NB)(b) and 2-F-4-nitroacetophenone (F-NAP)(c). F-ENB, F-NB and F-NAP by NfsB was performed in 50 mM Tris-HCl buffer (pH 7.4) containing 5 mM EDTA, and 40 μM NADH in a total reaction volume of 500 μL. The reaction was initiated by adding enzyme (22 nM) and the consumption of NADH was monitored at 340 nm. The k_{cat} and K_m values were determined by varying the concentration of F-ENB (10-100 μM), F-NB (40-1000 μM) and F-NAP (10-100 μM). Initial velocities as a function of substrate concentration were fitted to the Michaelis–Menten equation using GraphPad Prism 4. Each experiment was performed in triplicate and all the data points were included when the data were fit by the Michaelis–Menten equation.

The K_m values of F-ENB, F-NB and F-NAP were 28±8.0 μM, 686±174.3 μM and 37.6 ±5.4 μM, respectively, and the k_{cat} values of F-ENB, F-NB and F-NAP were 16.1±1.7, 12.4±1.6 s^{-1}**,** 18.8 ±1.1 s^{-1}, respectively.

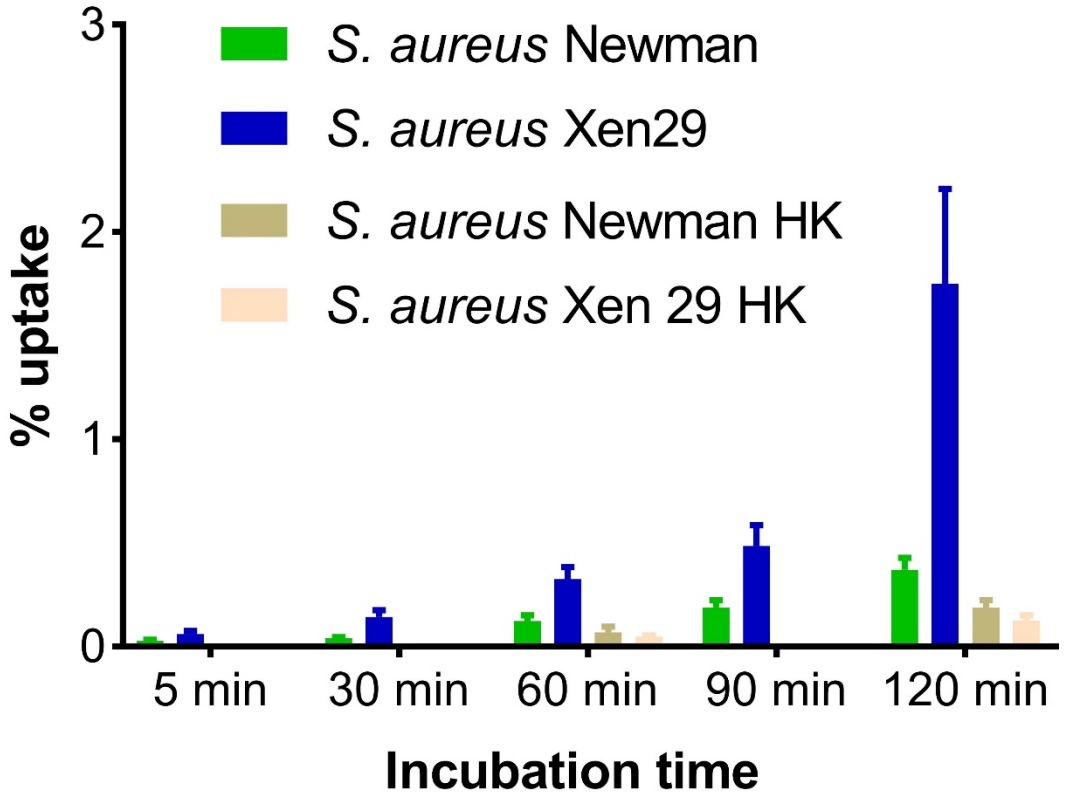

Figure S9. In vitro 2-[^{18}F]F-NB uptake by *S. aureus* Newman and Xen29. 1 μCi of 2-[^{18}F]F-NB was incubated in a 1 mL culture of *S. aureus* Newman (green bars) or *S. aureus* Xen29 (blue bars) for 5, 30, 60, 90 and 120 min. At both 60 and 120 min, there was significantly higher uptake in live *S. aureus* Newman and *S. aureus* Xen 29 compared to heat killed (HK) *S. aureus* strains.

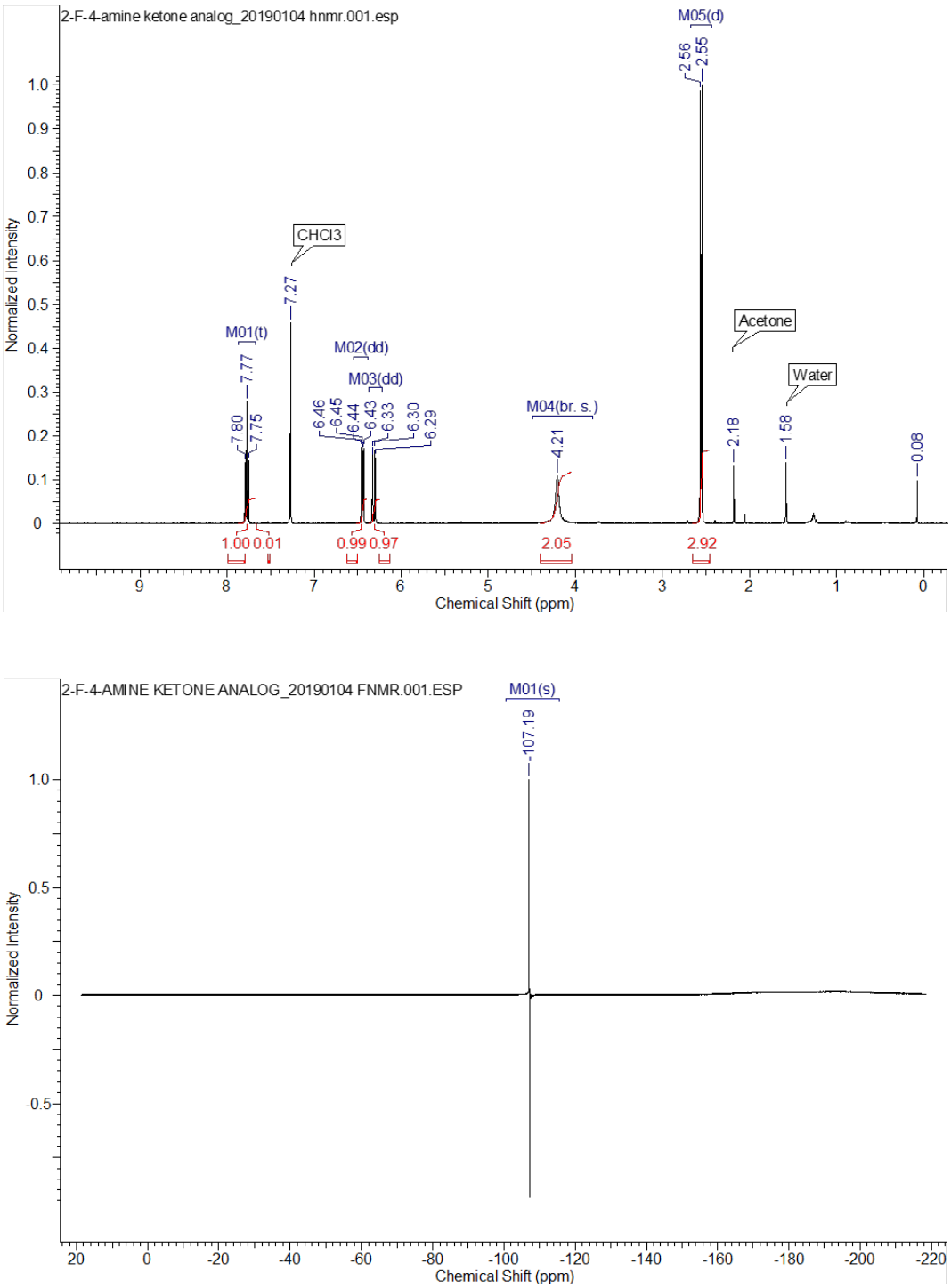

Figure S10. H-NMR and F-NMR of 2-F-4-aminoacetophenone

2-F-4-aminoacetophenone: ^{1}H NMR (400 MHz, CHLOROFORM-*d*) δ ppm 2.56 (d, *J*=5.38 Hz, 3 H) 4.21 (br. s., 2 H) 6.31 (dd, *J*=13.20, 2.20 Hz, 1 H) 6.44 (dd, *J*=8.56, 2.20 Hz, 1 H) 7.77 (t, *J*=8.56 Hz, 1 H). ^{19}F NMR (376 MHz, CHLOROFORM-*d*) δ ppm -107.19 (s, 1 F)